Polymer 50 (2009) 4007–4017

Contents lists available at ScienceDirect

Polymer

journal homepage: www.elsevier.com/locate/polymer

Crystallization, spherulite growth, and structure of blends of crystalline and amorphous poly(lactide)s

Leevameng Bouapao [a], Hideto Tsuji [a,*], Kohji Tashiro [b], Jianming Zhang [b,c], Makoto Hanesaka [b]

[a] Department of Ecological Engineering, Faculty of Engineering, Toyohashi University of Technology, Tempaku-cho, Toyohashi, Aichi 441-8580, Japan
[b] Department of Future Industry-oriented Basic Science and Materials, Graduate School of Engineering, Toyota Technological Institute, Hisakata, Tempaku, Nagoya 468-8577, Japan
[c] Key Laboratory of Rubber-plastics, Ministry of Education, Qingdao University of Science and Technology, Qingdao city 266042, People's Republic of China

ARTICLE INFO

Article history:
Received 5 March 2009
Received in revised form
2 June 2009
Accepted 18 June 2009
Available online 24 June 2009

Keywords:
Poly(lactide)
Crystallization
Polymer blending

ABSTRACT

The effects of incorporated amorphous poly(DL-lactide) (PDLLA) on the isothermal crystallization and spherulite growth of crystalline poly(L-lactide) (PLLA) and the structure of the PLLA/PDLLA blends were investigated in the crystallization temperature (T_c) range of 90–150 °C. The differential scanning calorimetry results indicated that PLLA and PDLLA were phase-separated during crystallization. The small-angle X-ray scattering results revealed that for T_c of 130 °C, the long period associated with the lamellae stacks and the mean lamellar thickness values of pure PLLA and PLLA/PDLLA blend films did not depend on the PDLLA content. This finding is indicative of the fact that the coexisting PDLLA should have been excluded from the PLLA lamellae and inter-lamella regions during crystallization. The decrease in the spherulite growth rate and the increase in the disorder of spherulite morphology with an increase in PDLLA content strongly suggest that the presence of a very small amount of PDLLA chains in PLLA-rich phase disturbed the diffusion of PLLA chains to the growth sites of crystallites and the lamella orientation. However, the wide-angle X-ray scattering analysis indicated that the crystalline form of PLLA remained unvaried in the presence of PDLLA.

1. Introduction

Poly(lactide) (PLA) has stereoisomers, such as poly(L-lactide) (PLLA), poly(D-lactide) (PDLA), and poly(DL-lactide) (PDLLA). Isotactic and optically active PLLA and PDLA are crystalline, whereas relatively atactic and optically inactive PDLLA is amorphous. PLLA and PDLA crystallize in pseudo-orthorhombic unit cell with 10_3 helical conformation [1]. Isothermal crystallization and spherulite growth of PLLA from the melt has been intensively investigated [1–12].

Fischer et al. [2] and Kalb and Pennings [3] observed the spherulite formation of PLLA. Vasanthakumari and Pennings [4], Abe et al. [5], Miyata and Masuko [6], Wang and Mano [7], and Tsuji et al. [8–10] investigated the effects of molecular weight and crystallization temperature (T_c) on the radius growth rate (G) and morphology of PLLA spherulites and crystallite assemblies and carried out kinetic analysis. Di Lorenzo [11] and Yasuniwa et al. [12] studied the effect of T_c on overall crystallization behavior of PLLA. Zhang et al. [13,14] surveyed the intermolecular interaction, the structural change, and the crystallization dynamics during crystallization by the use of infrared and two-dimensional infrared correlation spectroscopy. Huang et al. [15] and Tsuji et al. [16] reported that the lamellar stacks (L) values increased with increasing T_c. Recently, Pan et al. [17], Kawai et al. [18], and Zhang et al. [19] found that the transition of α' to α form of PLLA occurs at T_c of 110–120 °C, whereas Yasuniwa et al. showed that the transition of α' to α form of PLLA occurs at T_c of 155–165 °C [20].

On the other hand, blending of crystalline PLLA or PDLA with amorphous PDLLA is effective for controlling the overall crystallinity (X_c) [21–23] and hydrolytic degradation rate [23]. The crystallization of PLLA takes place in the PLLA/PDLLA blends from the melt at the PLLA content higher than 0.2 and spherulites are formed at the PLLA content exceeding 0.6 [21,22]. The X_c of PLLA is practically constant in PLLA/PDLLA blends at PLLA content above 0.6 [21]. Xu et al. reported that the presence of PDLLA led to reduced G and band spacing of PLLA spherulites [25]. Recently, Urayama et al. utilized the crystalline and amorphous PLA with high and low L-lactyl units of 99 and 77%, respectively, and showed that overall X_c decreased with increasing the amorphous PLA content [26]. Moreover, Tsuji and Ikada studied the hydrolytic degradation of PDLA or PDLA/PDLLA blends, and found that PDLLA was predominantly degraded and removed from the blends and, thereby, the

* Corresponding author.
E-mail address: tsuji@eco.tut.ac.jp (H. Tsuji).

0032-3861/$ – see front matter © 2009 Elsevier Ltd. All rights reserved.
doi:10.1016/j.polymer.2009.06.040

degradation rate of blends was elevated by the incorporation of PDLLA [23]. Besides, the single T_g observed for PLLA/PDLLA blends [24,27] and PLLA/L-lactide-rich PLA blends [19] showed that these two polymers are miscible. In contrast, Kairong et al. [28] reported that PLLA and PDLLA became phase-separated in their blends by low temperature annealing (or storage) at 0 °C.

As mentioned above, most of the studies in the past focused on the effect of amorphous PDLLA on the hydrolysis, X_c, and G of PLLA. However, as far as we are aware, there has been no information about the behavior of incorporated PDLLA and the structural change of PLLA/PDLLA blends at different blending ratios during the crystallization and spherulite growth of PLLA. Therefore, the purpose of the present study is to investigate the effect of incorporated PDLLA on the crystallization and spherulite growth rate of PLLA and the structural change of PLLA/PDLLA blends at different blending ratios. For this purpose, the PLLA/PDLLA blends were prepared to have different PLLA contents, and the long period, crystallinity, and crystalline thickness, crystalline form, G, and induction period for spherulite formation (t_i) were studied by the use of differential scanning calorimetry (DSC), wide-angle X-ray scattering (WAXS), small-angle X-ray scattering (SAXS), and polarized optical microscopy (POM).

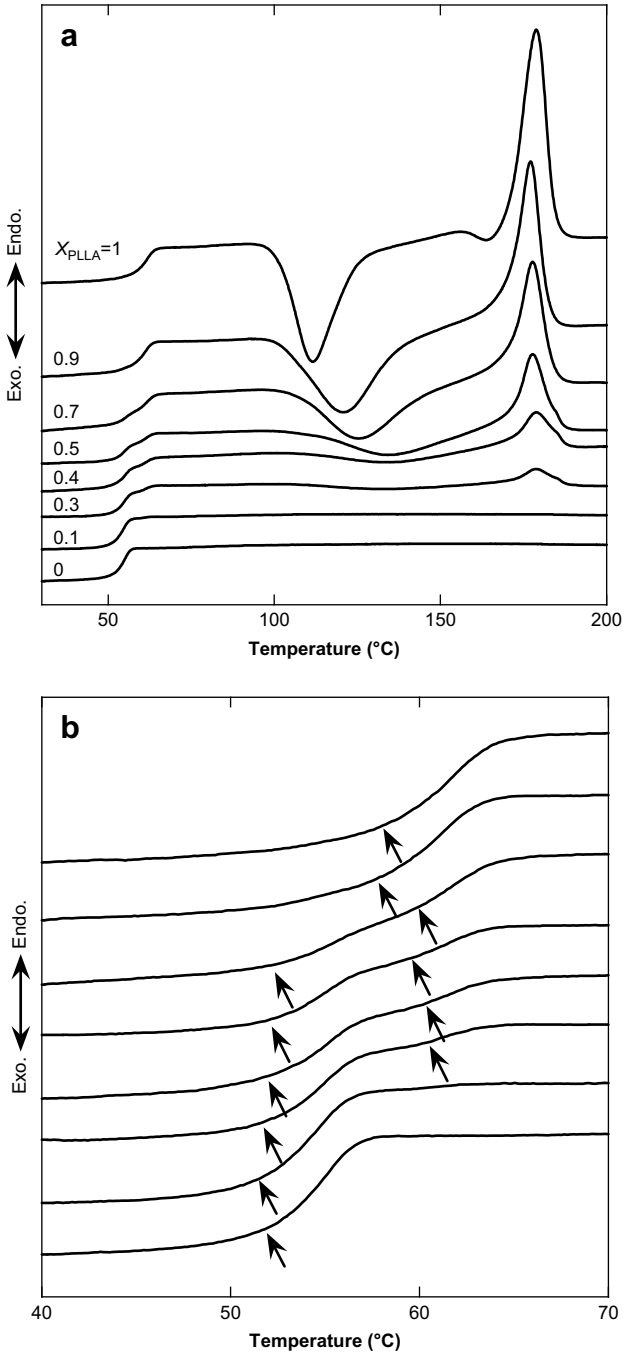

Fig. 1. DSC thermograms of melt-quenched pure PLLA, PDLLA, and blend films (a) and their magnified glass transition peaks (b). The arrows show T_g values.

2. Experimental section

2.1. Materials

PLLA [weight-average molecular weight (M_w) = 5.2×10^5 g mol^{-1}, M_w/number-average molecular weight (M_n) = 1.8] and PDLLA ($M_w = 5.2 \times 10^5$ g mol^{-1}, $M_w/M_n = 1.7$) were purchased from Polysciences Inc. (Washington, Pennsylvania, USA). PLLA and PDLLA were purified by reprecipitation using dichloromethane and acetone as the solvents, respectively, and methanol as the precipitant. Pure PLLA, PDLLA, and blend films (thickness of 20 μm) with different PLLA contents [$X_{PLLA} = W_{PLLA}/(W_{PLLA} + W_{PDLLA})$, where W_{PLLA} and W_{PDLLA} are weights of PLLA and PDLLA, respectively] were prepared by casting 1 g dL^{-1} solutions of the polymers using dichloromethane as the solvent, and subsequent solvent evaporation at room temperature (25 °C) for approximately two days, followed by drying in vacuum for 7 days [29,30].

For preparation of melt-quenched and crystallized specimens, pure PLLA, PDLLA, and their blend films were sealed in test tubes under reduced pressure, melted at 200 °C for 3 min, and quenched at 0 °C for 5 min (melt-quenched specimens) or crystallized at T_c of 130 °C for 10 h, and quenched at 0 °C for 5 min (crystallized specimens).

For WAXS measurements, the pure PLLA and blend films with $X_{PLLA} = 0.5$ (thickness of 100 μm) were prepared, and for SAXS measurements, the pure PLLA, PDLLA, and blend films (thickness of 500 μm) were fabricated by melting at 200 °C for 3 min, crystallization at different T_c of 80–150 °C for 10 h, and quenching at 0 °C.

2.2. Physical measurements and optical observation

The M_w and M_n of the polymers were evaluated in chloroform at 40 °C by a Tosoh (Tokyo, Japan) GPC system (refractive index monitor: RI-8020) with two TSK Gel columns (GMH_{xL}) using polystyrene standards. Glass transition, cold crystallization, and melting temperatures (T_g, T_{cc}, and T_m, respectively) and enthalpies of cold crystallization and melting (ΔH_{cc} and ΔH_m, respectively) of

Table 1
Thermal properties of melt-quenched pure PLLA, PDLLA, and blend films.

X_{PLLA}[a]	T_g[b] (°C)	T_{cc}[b] (°C)	T_m[b] (°C)	ΔH_{cc}[c] (J g^{-1})	ΔH_m[c] (J g^{-1})	ΔH(total)[d] (J g^{-1})
1	57.9	111.6	178.8	−38.2	38.6	0.4
0.9	57.5	120.9	177.4	−34.6	34.6	0.0
0.7	52.4, 60.0	125.3	178.3	−25.2	25.5	0.3
0.5	52.2, 59.6	134.3	178.2	−15.1	15.2	0.1
0.4	52.0, 60.3	135.3	179.5	−7.6	−8.0	0.4
0.3	51.8, 60.6	132.2	179.3	−3.4	−3.5	0.1
0.1	51.6	0	0	0	0	0
0	51.9	0	0	0	0	0

[a] $X_{PLLA} = W_{PLLA}/(W_{PLLA} + W_{PDLLA})$, where W_{PLLA} and W_{PDLLA} are weights of PLLA and PDLLA, respectively.
[b] The glass transition, cold crystallization, and melting temperatures (T_g, T_{cc}, and T_m, respectively) were estimated by DSC.
[c] Enthalpies of cold crystallization and melting (ΔH_{cc} and ΔH_m, respectively).
[d] $\Delta H(\text{total}) = \Delta H_{cc} + \Delta H_m$.

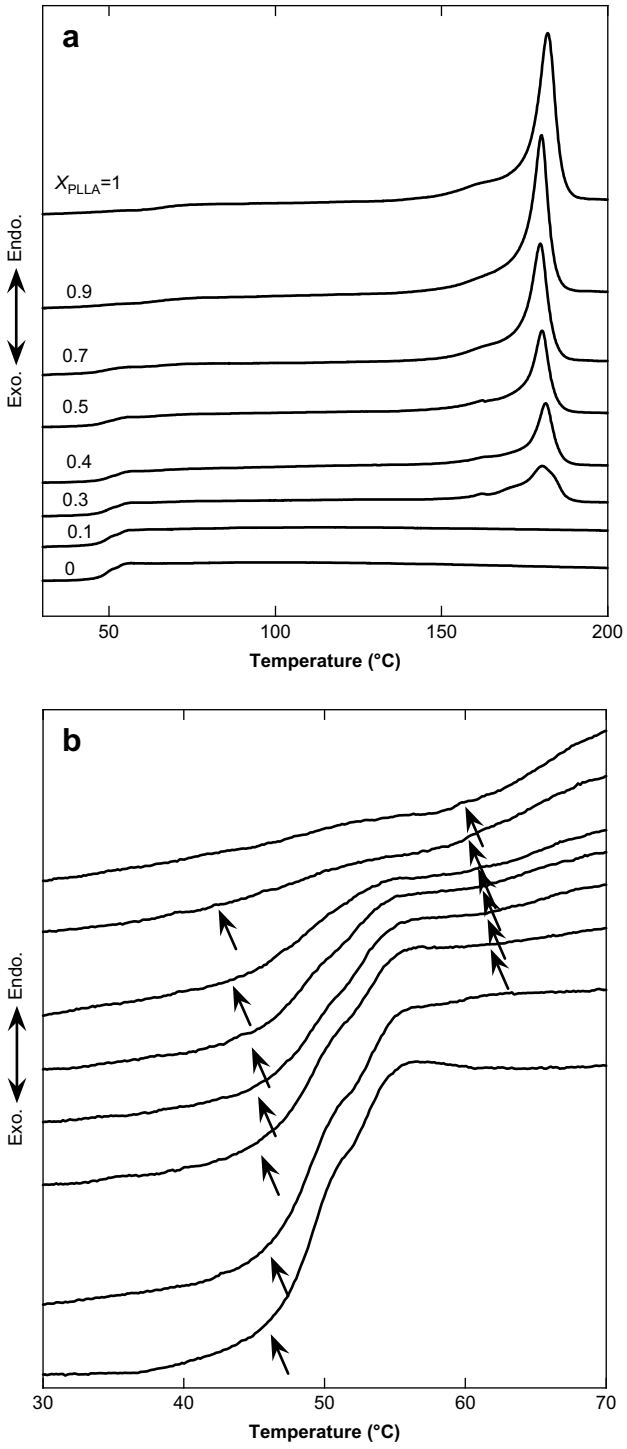

Fig. 2. DSC thermograms of pure PLLA, PDLLA, and blend films crystallized isothermally at T_c of 130 °C for 10 h (a) and their magnified glass transition peaks (b). The arrows show T_g values.

crystallized films were determined with a Shimadzu (Kyoto, Japan) DSC-50 differential scanning calorimeter with a cooling cover (LTC-50). The specimens (about 3 mg) were heated from 0 to 200 °C at a rate of 10 °C min^{-1} under a nitrogen gas flow at a rate of 50 ml min^{-1}. The T_g, T_{cc}, T_m, ΔH_{cc} and ΔH_m values were calibrated using tin, indium, and benzophenone as standards. The crystallinity (X_c) of crystallized films were calculated according to the following equations [29]:

Table 2
Thermal properties of pure PLLA, PDLLA, and blend films crystallized at T_c of 130 °C for 10 h.

X_{PLLA}[a]	T_g[b] (°C)	T_m[b] (°C)	ΔH_m[c] (J g^{-1})	Non-normalized		Normalized
				X_c(DSC) (%)	X_c(WAXS) (%)	X_c(DSC) (%)
1	60.2	180.7	55.5	59.7	58.7	59.7
0.9	42.4, 60.3	179.2	49.8	53.5	55.8	59.5
0.7	43.5, 60.9	179.2	39.1	42.0	45.1	60.1
0.5	44.8, 61.2	179.9	27.7	29.8	33.7	59.6
0.4	45.3, 61.5	180.2	20.5	22.0	26.5	55.1
0.3	45.5, 61.8	179.8	16.0	17.2	18.8	57.3
0.1	46.2	–	–	0	0	–
0	46.2	–	–	0	0	–

[a] $X_{PLLA} = W_{PLLA}/(W_{PLLA} + W_{PDLLA})$, where W_{PLLA} and W_{PDLLA} are weights of PLLA and PDLLA, respectively.
[b] T_g and T_m are glass transition and melting temperatures, respectively.
[c] Enthalpy of melting.

$$\text{Non-normalized } X_c(\text{DSC})\ (\%) = 100\Delta H_m/\Delta H_m^0 \quad (1)$$

$$\text{Normalized } X_c(\text{DSC})\ (\%) = \text{Non-normalized } X_c(\text{DSC})/X_{PLLA} \quad (2)$$

where ΔH_m^0 is the enthalpy of melting of PLLA crystal having an infinite thickness. We used the value of 93 J g^{-1} reported by Fischer et al. as ΔH_m^0 [2], because it gave the X_c values comparable to those obtained by WAXS measurements.

The spherulite growth in the films (thickness of ca. 20 μm) was observed by an Olympus (Tokyo, Japan) polarization microscope (BX50) equipped with a heating–cooling stage and temperature controller (Linkam LK-600PM) under a constant nitrogen gas flow. The crystallization of the films was performed as follows. The films were first heated at a rate of 100 °C min^{-1} from room temperature to 200 °C, held at the same temperature for 3 min to erase thermal history, cooled at a rate of 100 °C min^{-1} to an arbitrary T_c in the range of 90–150 °C, and then held at the same T_c (spherulite growth was observed here). Here, we don't show the G values at T_c lower

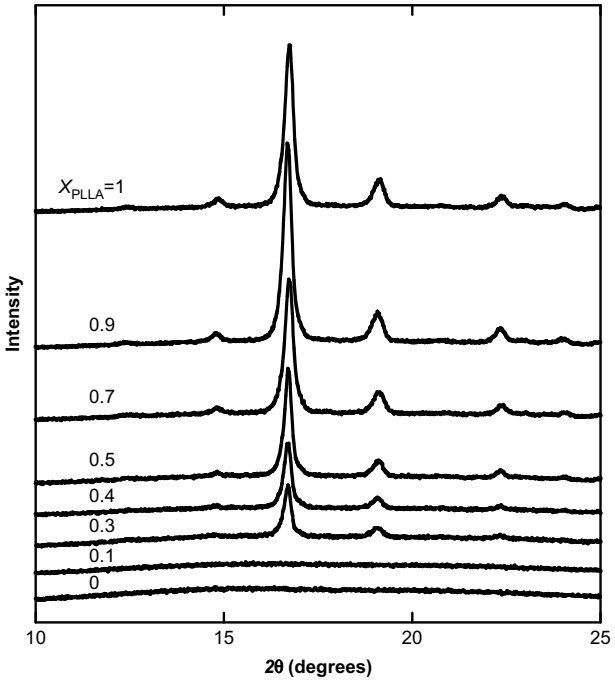

Fig. 3. WAXS profiles of pure PLLA, PDLLA, and blend films crystallized isothermally at T_c of 130 °C for 10 h.

than 90 °C, because the G values were too small to be evaluated. WAXS measurements were carried out with a Rigaku (Tokyo, Japan) RINT-2500 equipped with a Cu-Kα source ($\lambda = 1.542$ Å). The X_c values of crystallized films were estimated by WAXS measurements using the following equation:

$$\text{Non-normalized } X_c(\text{WAXS})\ (\%) = 100S_c/(S_c + S_a) \quad (3)$$

where S_c and S_a are crystalline and amorphous diffraction peak areas, respectively. Here, we did not calculate the normalized X_c (WAXS) values, due to the difficulty to separate the diffraction of amorphous region of crystalline PLLA from that of amorphous PDLLA.

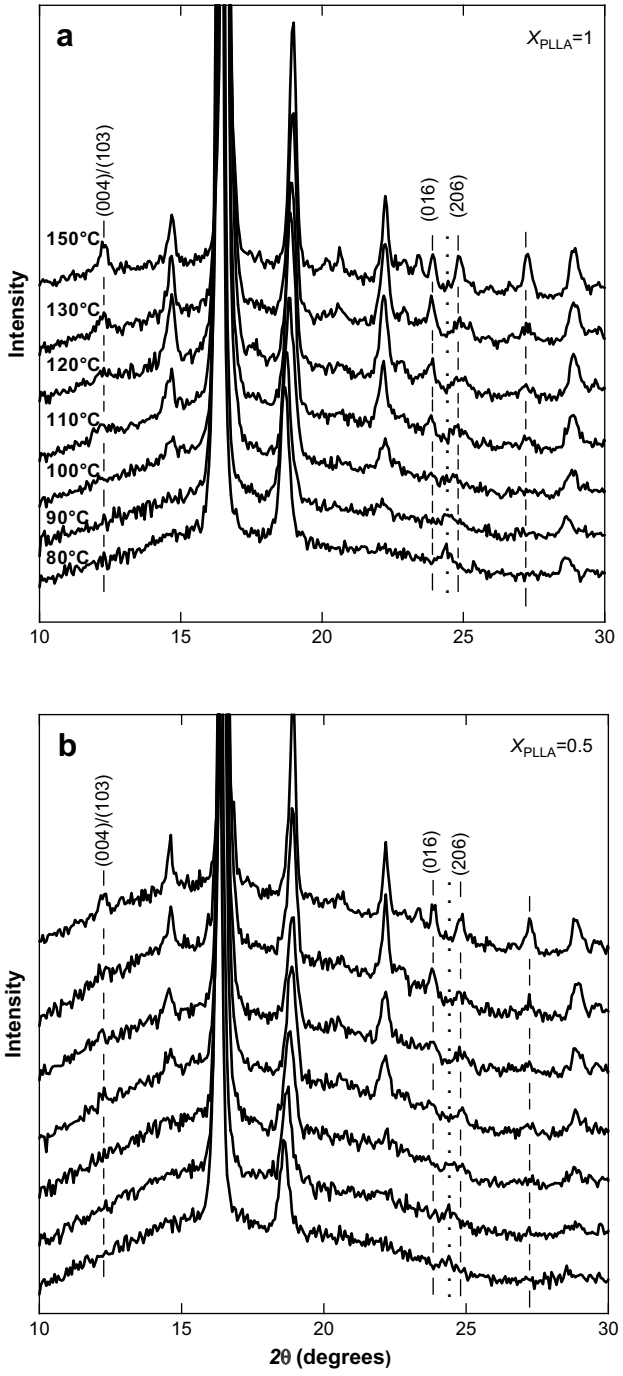

Fig. 4. WAXS profiles of pure PLLA film (a) and blend film with $X_{PLLA} = 0.5$ (b) crystallized isothermally at different T_c values of 80–150 °C for 10 h.

SAXS measurements were performed using a Rigaku X-ray diffractometer Nanoviewer. The incident X-ray beam was graphite-monochromatized Cu-Kα line which was focused onto the sample position using a confocal mirror. The 2-dimensional SAXS images were recorded using an Imaging Plate Detector as well as a 2D detector Pilatus (Dectris, Rigaku). The SAXS data were collected in the range of $0 \le q \le 1.0$ Å^{-1} ($q = 4\pi/\lambda \sin\theta$), where q is the scattering vector, λ is the X-ray wavelength, and θ is half of the scattering angle.

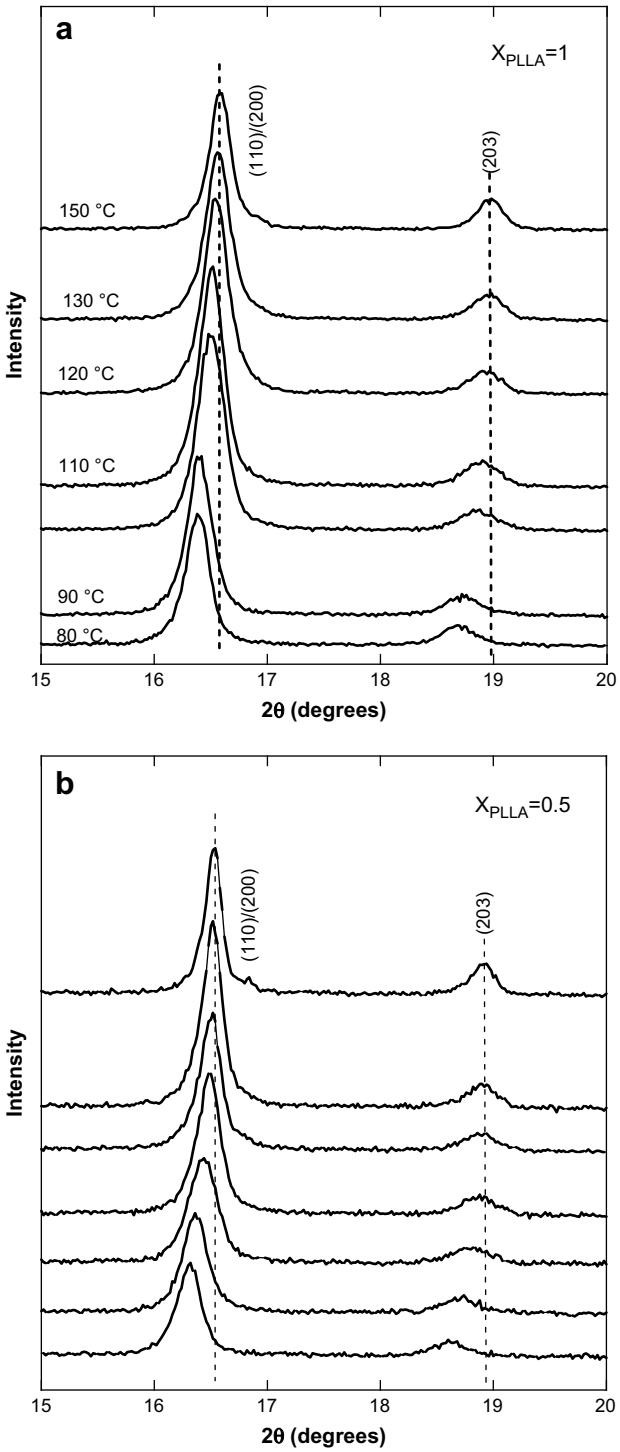

Fig. 5. WAXS profiles for (110)/(200) and (203) lattice planes of pure PLLA film (a) and blend film with $X_{PLLA} = 0.5$ (b) crystallized isothermally at different T_c values of 80–150 °C for 10 h.

3. Results and discussions

3.1. Non-isothermal crystallization

To investigate non-isothermal crystallization of melt-quenched specimens during heating, their DSC measurements were carried out with the conditions stated in the Experimental section. Fig. 1 shows the DSC thermograms of melt-quenched pure PLLA, PDLLA, and their blend films. The thermal properties of these films were estimated from Fig. 1 and are shown in Table 1. Total enthalpy [ΔH(total)] was calculated from ΔH_{cc} in the temperature range of 100–150 °C and ΔH_m in the temperature range of 150–190 °C according to the following equation:

$$\Delta H(\text{total}) = \Delta H_{cc} + \Delta H_m \quad (4)$$

Here, by definition, ΔH_{cc} is negative and ΔH_m is positive. As seen in

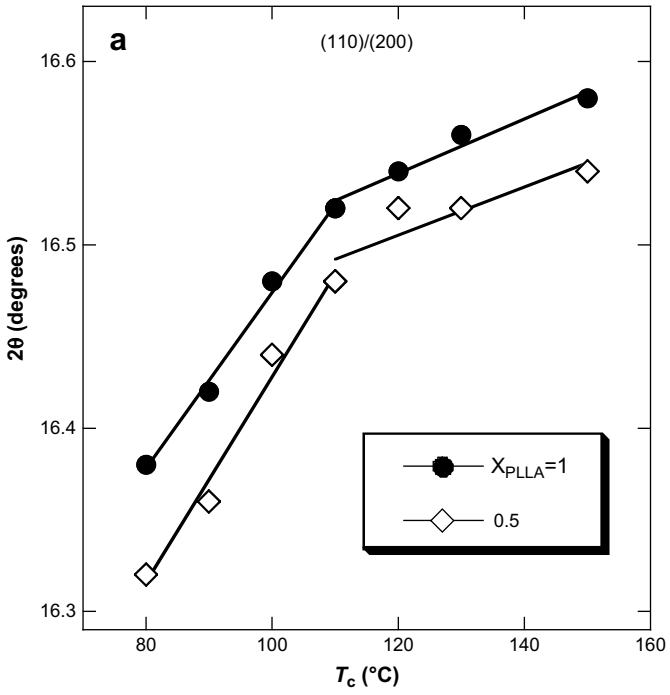

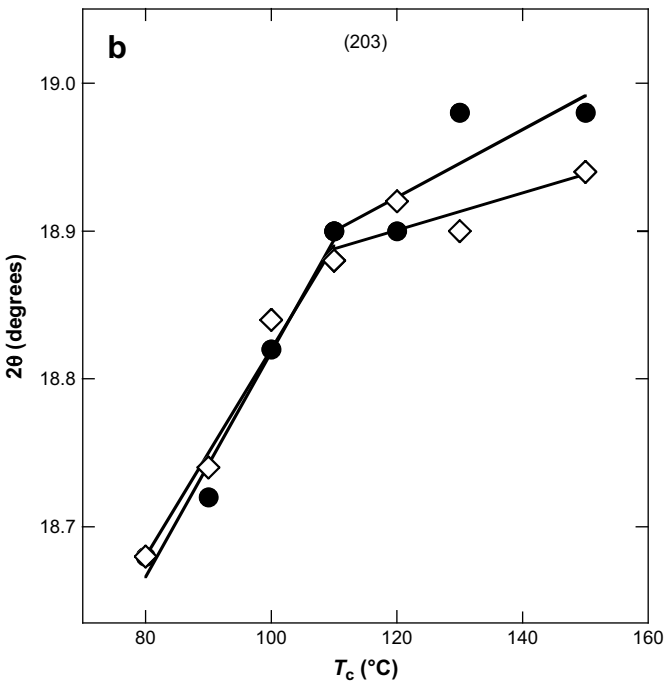

Fig. 6. 2θ values of (110)/(200) (a) and (203) (b) lattice planes of pure PLLA film and blend film with $X_{PLLA} = 0.5$ as a function of T_c.

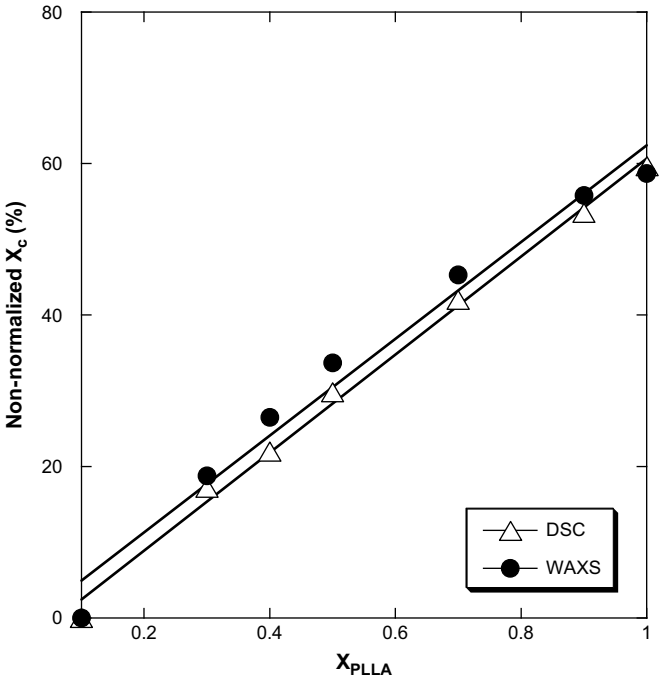

Fig. 7. Non-normalized crystallinity (X_c) estimated by DSC measurements and X-ray diffractometry of pure PLLA and blend films crystallized isothermally at T_c of 130 °C for 10 h.

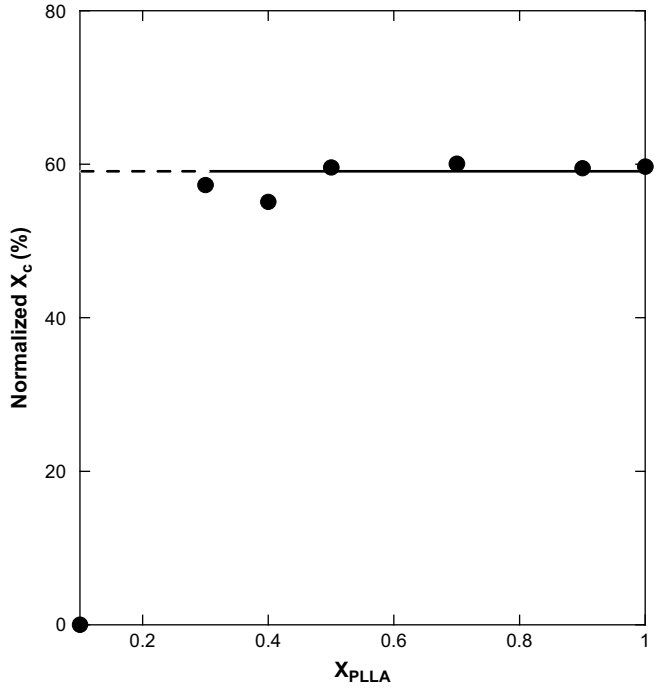

Fig. 8. Normalized crystallinity (X_c) estimated by DSC measurement of pure PLLA and blend films crystallized isothermally at T_c of 130 °C for 10 h.

Table 1, the ΔH(total) values of all the films were almost zero, indicating that they were amorphous before crystallization (DSC heating).

As seen in Fig. 1(b) and Table 1, the two glass transitions were observed for the blend films with $X_{PLLA} = 0.3$–0.9 at constant temperatures around 50 and 60 °C, which are in agreement with the T_g values of pure PDLLA and PLLA films, respectively. These findings are indicative of the fact that PLLA and PDLLA are immiscible with each other and were phase-separated before crystallization. Interestingly, the T_{cc} values of the blend films (above $X_{PLLA} = 0.3$) increased monotonously from 112 to 135 °C with decreasing X_{PLLA}. This reveals that the very small amount of PDLLA chains present in PLLA-rich phase delayed the crystallization of PLLA. However, the melting peaks were observed at a constant temperature around 180 °C for the pure PLLA and blend films with X_{PLLA} above 0.3. This indicates that the incorporated PDLLA did not vary the final crystalline thickness of PLLA. On the other hand, neither cold crystallization peak nor melting peak was observed for the blend and PDLLA films with X_{PLLA} below 0.1, revealing that they are not crystallizable.

3.2. Isothermal crystallization

3.2.1. Differential scanning calorimetry

Fig. 2 shows the DSC thermograms of pure PLLA, PDLLA, and their blend films crystallized isothermally at T_c of 130 °C for 10 h. The thermal properties of these films were estimated from Fig. 2 and are shown in Table 2. As seen in Table 2 and Fig. 2(b), the two glass transitions were observed for the blend films with $X_{PLLA} = 0.3$–0.9 at constant temperatures around 45 and 60 °C, which are in complete agreement with the T_g values of pure PDLLA and PLLA films, respectively. The same result was obtained for melt-quenched blend films before crystallization (Fig. 1). These findings are indicative of the fact that PLLA and PDLLA are immiscible with each other and were phase-separated during crystallization. The T_m was observed at a constant temperature around 180 °C for the pure PLLA and blend films with X_{PLLA} above 0.3, in good agreement with the results of melt-quenched blend films (Fig. 1) and the reported result [28]. This indicates that PLLA was crystallizable in the presence of PDLLA at X_{PLLA} of 0.3–1 and suggests that the incorporated PDLLA did not vary the crystalline thickness of PLLA. On the other hand, no melting peaks were observed for the blend and PDLLA films with X_{PLLA} below 0.1.

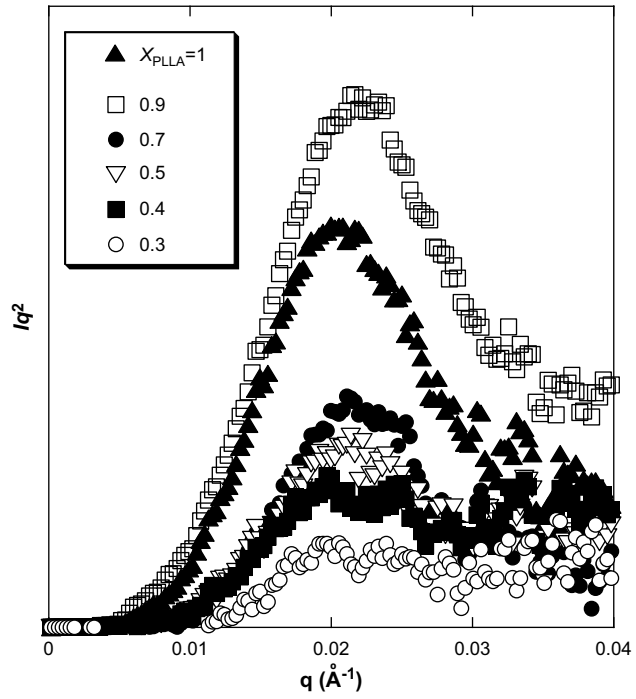

Fig. 9. SAXS profiles of pure PLLA and blend films crystallized isothermally at T_c of 130 °C for 10 h.

Table 3
Structural parameters of pure PLLA and blend films crystallized at T_c of 130 °C for 10 h.

X_{PLLA}[a]	q_{max}[b] (Å^{-1})	$L(q_{max})$[c] (Å)	Q[d]	$\langle d\rangle$[e] (Å)	L[f] (Å)	l_a[g] (Å)	w_c[h]
1	0.0196	320.6	1.36	104.6	311.1	206.5	0.336
0.9	0.0211	297.8	1.39	107.4	281.5	174.1	0.382
0.7	0.0220	285.6	1.39	108.3	288.9	180.6	0.375
0.5	0.0205	306.5	1.37	108.3	320.4	212.1	0.338
0.4	0.0198	317.3	1.35	110.2	321.3	211.1	0.343
0.3	0.0203	309.5	1.42	113.0	307.4	194.4	0.366

[a] $X_{PLLA} = W_{PLLA}/(W_{PLLA} + W_{PDLLA})$, where W_{PLLA} and W_{PDLLA} are weights of PLLA and PDLLA, respectively.
[b] The maximum scattering vector.
[c] Long period, $L(q_{max}) = 2\pi/q_{max}$.
[d] The invariant.
[e] The mean lamellar thickness.
[f] Long period obtained from one-dimensional correlation function.
[g] Thickness of amorphous part, $l_a = L(1 - w_c)$.
[h] Linear crystallinity, $w_c = \langle d\rangle/L$.

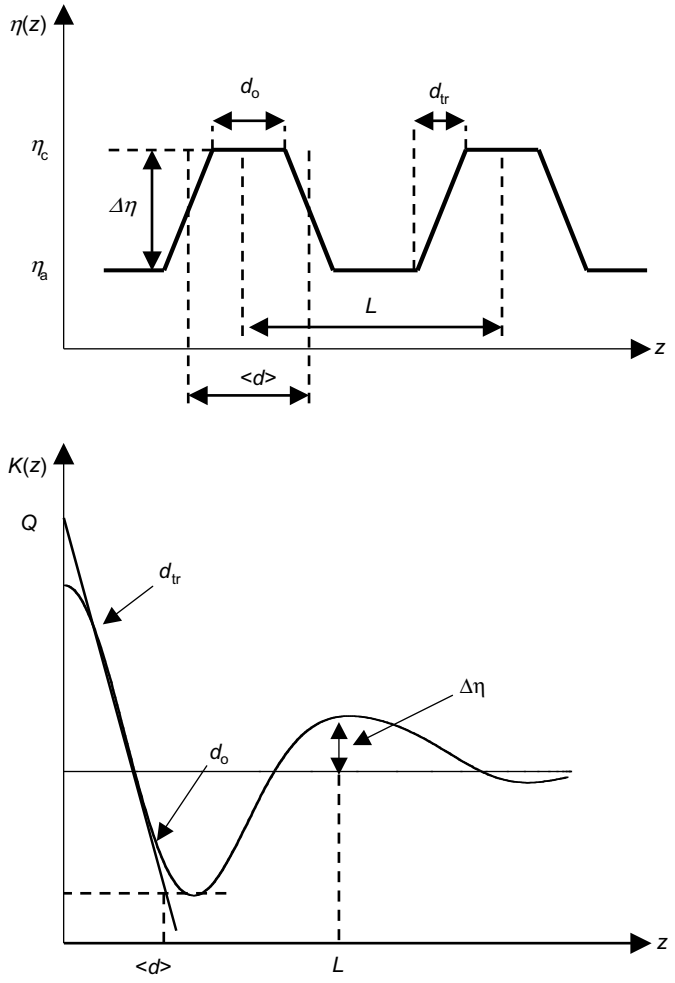

Fig. 10. The electron density $\eta(z)$ and electron density correlation function $K(z)$ distribution for the lamellar system. Q: the invariant, d_{tr}: thickness of the transition zone between the crystalline and amorphous part, d_o: thickness of lamellar core, $\langle d\rangle$: mean lamellar thickness, L: long period, η_c and η_a: electron density of crystalline and amorphous parts, respectively, and $\Delta\eta$: electron density difference between crystalline lamella and amorphous parts.

3.2.2. Wide-angle X-ray scattering

Fig. 3 shows the WAXS profiles of the pure PLLA, PDLLA, and their blend films crystallized isothermally at T_c of 130 °C for 10 h. The sharp crystalline peaks were observed at 2θ values of around 17 and 19° for the pure PLLA and blend films with X_{PLLA} above 0.3. These two peaks are attributed to the diffraction from (110)/(200) and (203) lattice planes, respectively, and are characteristic of the α′- and α-forms of PLLA, in good agreement with the reported results [17–19]. On the other hand, no diffraction peaks were observed for X_{PLLA} below 0.1, indicating that they are amorphous, in consistent with the result obtained by DSC measurements (Figs. 1 and 2). We have evaluated the half width values of pure PLLA and blend films, and found that these values were constant, irrespective X_{PLLA}, suggesting that the crystalline size of pure PLLA remained unvaried in the presence of PDLLA.

To elucidate the formation of crystalline species of α′- and α-forms at different T_c values, the pure PLLA film and the blend film with $X_{PLLA} = 0.5$ prepared by aforementioned casting method were crystallized from the melt at different T_c values in the range of 80–150 °C for 10 h and their WAXS profiles were obtained (Figs. 4 and 5). As reported, α′- and α-forms are formed at relatively low and high T_c values [17–19]. Pan et al. [17], Kawai et al. [18] and Zhang et al. [19] showed that the transition from α′- to α-form takes place at T_c of 110 and 120 °C. The slight difference in the transition temperature of PLLA from α′- to α-form between the literatures should be due to the difference in molecular weight or crystallization procedure. As seen in Fig. 4, for the pure PLLA and blend films crystallized at $T_c \geq 110$ °C, some weak peaks appear at 2θ values of 12.5, 24.0, 25.0, and 27.5° (broken lines), whereas such peaks were not observed for the samples crystallized at $T_c < 110$ °C. These 2θ values are in good agreement with those reported for α-form [17,18]. On the other hand, the peak at 2θ value of 24.4° (dotted line), which is characteristic of α′-form [17], was only observed for the samples crystallized at $T_c < 110$ °C. The 2θ values of (110)/(200) and (203) lattice planes were obtained from Fig. 5 and are plotted in Fig. 6 as a function of T_c. The slopes of 2θ values became smaller for T_c above 110 °C. From above reasons, it is strongly suggested that the transition from α′- to α-form of PLLA occurred in the pure PLLA and blend films at around T_c of 110 °C and the transition temperature remained unvaried in the presence of PDLLA.

Fig. 7 shows the non-normalized X_c(DSC) and X_c(WAXS) of the pure PLLA and blend films crystallized isothermally at T_c of 130 °C for 10 h. For X_c(DSC) values, as explained in the Experimental section, we used the value of 93 J g^{-1} reported by Fischer et al. as ΔH^0_m [2], because it gave the X_c values comparable to those obtained by WAXS measurements. As seen in Fig. 7, the X_c values obtained by different methods are similar with each other, and increased linearly with increasing X_{PLLA}. Fig. 8 shows the normalized X_c(DSC) of the pure PLLA and blend films. The normalized X_c(DSC) values were practically constant for $X_{PLLA} = 0.3$–1, in agreement with the previously reported result [21]. This indicates that the coexisting PDLLA did not influence the normalized X_c of PLLA for X_{PLLA} above 0.3 after the completion of crystallization. On the other hand, the normalized X_c(DSC) values were practically zero for $X_{PLLA} = 0.1$, reflecting that PLLA could not crystallize in the presence of a large amount of PDLLA. The large amount of PDLLA surrounding PLLA should have disturbed the formation of PLLA crystallite nuclei or the growth of PLLA crystallites in the limited crystallization period of 10 h.

3.2.3. Small-angle X-ray scattering

Fig. 9 shows the SAXS profiles of the pure PLLA and blend films crystallized isothermally at T_c of 130 °C for 10 h. The q_{max} values obtained from this figure are summarized in Table 3. As seen in

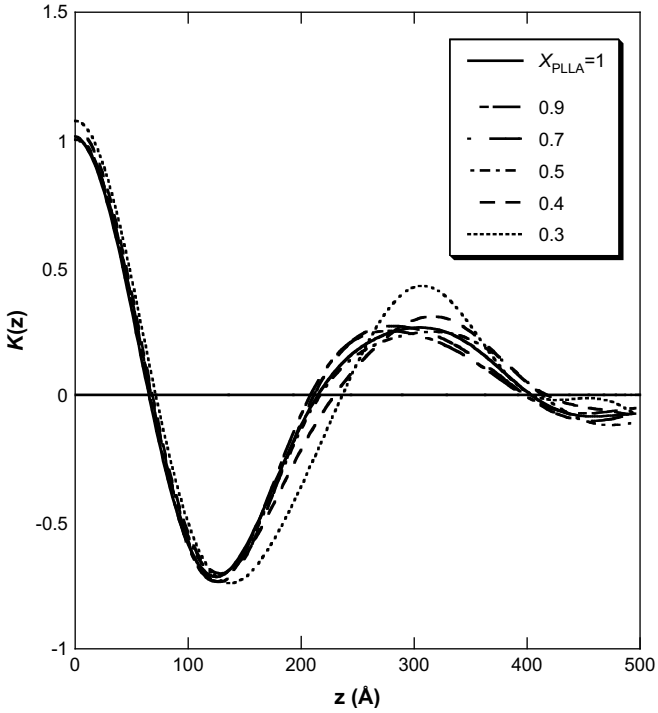

Fig. 11. One-dimensional correlation function for pure PLLA and blend films crystallized isothermally at T_c of 130 °C for 10 h.

Table 3, for the films with X_{PLLA} above 0.3, the intensity gave maxima at the q_{max} values of 0.196–0.220, which are practically constant, irrespective X_{PLLA}. On the other hand, no explicit peaks were observed for the films with X_{PLLA} below 0.1, revealing that they were amorphous, in consistent with the results obtained by DSC and WAXS measurements (Figs. 1–3). Fig. 10 illustrates a typical electron density correlation function [$K(z)$] and the electron density distribution $\eta(z)$ for the lamellar system. Under the assumption of the two-phase model consisting of the alternately stacked structure of the crystalline and amorphous layers, the $K(z)$ is defined by the following equation and can be calculated from SAXS data [31,32]:

$$K(z) = \langle[\eta(z') - \langle\eta\rangle][\eta(z+z') - \langle\eta\rangle]\rangle = 2\pi^{-1}\int_0^\infty q^2 I(q)\cos(qz)\mathrm{d}q \quad (5)$$

where $\langle\ \rangle$ means the statistical average and $\eta(z)$ and $\langle\eta\rangle$ are the electron density variation along the lamellar normal and the mean electron density, respectively, $I(q)$ is the experimental SAXS intensity at a given q, and z is the correlation distance. Various points indicated on the $K(z)$ curve give various physical parameters. In Fig. 10, $Q = \pi^{-1}\int_0^\infty q^2 I(q)\mathrm{d}q$ is invariant, $\langle d\rangle$ is the mean lamellar thickness, d_{tr} is the mean boundary thickness, d_o is the mean core thickness, and L is the long spacing [31,32]. $K(z)$ was calculated from the SAXS data (Fig. 9) and plotted in Fig. 11. The Q, $\langle d\rangle$, L, the linear crystallinity (w_c) ($w_c = \langle d\rangle/L$), and the thickness of amorphous (l_a) [$l_a = L(1 - w_c)$] values of the pure PLLA and blend films obtained from Fig. 11 are tabulated in Table 3.

As seen in Table 3, the obtained L values from one-dimensional correlation function of blend films with $X_{PLLA} = 0.3$–0.9 were 282–321 Å, which are practically constant, irrespective of X_{PLLA}, and are similar to 311 Å of the pure PLLA film. In addition, the obtained L values are in complete agreement with 286–317 Å for the blend films with $X_{PLLA} = 0.3$–0.9 obtained from q_{max} using the equation,

$L(q_{max}) = 2\pi/q_{max}$. These results mean that the L values were not influenced by the presence of PDLLA. The L values obtained in the present study are higher than 190–240 Å reported by Huang et al. for PLLA film ($M_w = 1.3 \times 10^5$ g mol^{-1}) crystallized at $T_c = 120$–148 °C [15], 217 Å reported by Kawai et al. for PLLA ($M_w = 2.1 \times 10^5$ g mol^{-1}) crystallized at $T_c = 120$ °C [18], 200–250 Å reported by Baratian et al. for PLLA ($M_w = 1.3 \times 10^5$ g mol^{-1}) crystallized at T_c of 120–145 °C [33], 180 Å reported by Cho et al. for PLLA ($M_w = 1.3 \times 10^5$ g mol^{-1}) crystallized at $T_c = 123$ °C [34], but are similar to 220–350 Å reported by Tsuji et al. for PLLA film ($M_w = 9.4 \times 10^5$ g mol^{-1}) crystallized at $T_c = 120$–160 °C [16]. The former result may be due to the fact that the molecular weight of PLLA used in the present study ($M_w = 5.2 \times 10^5$ g mol^{-1}) is higher than those in the previous literature ($M_w = 1.3 \times 10^5$, 2.1×10^5, 1.3×10^5, and 1.3×10^5 g mol^{-1}, respectively) [15,18,33,34]. The schematic representation of structural models of the pure PLLA and blend films are presented in Fig. 12. The SAXS results showed that the L values in the blend films were practically constant. The T_m values ($\langle d \rangle$ values) of the blend films were practically constant, irrespective of X_{PLLA} (Tables 1 and 2). In addition, as mentioned above, PLLA and PDLLA are immiscible with each other and were phase-separated before and after crystallization on the basis of two constant T_g values at different X_{PLLA} (Figs. 1 and 2). Therefore, it seems reasonable that PDLLA chains were excluded from the PLLA lamellae and the inter-lamella regions, as illustrated in the "Excluded model" of Fig. 12b. As far as we are aware, this result is the first report regarding the exclusion of amorphous relatively atactic polymer from the inter-lamella region of crystalline isotactic polymer having the same monomer units. In this model, $\langle d \rangle$ and l_a values are not influenced by the presence of PDLLA and its content. Moreover, as seen in Table 3, the w_c values obtained from one-dimensional correlation function of pure PLLA and blend films with X_{PLLA} above 0.3 were almost constant, irrespective of X_{PLLA}, in agreement with the result that the normalized X_c(DSC) values are invariable (Table 2), although the normalized X_c (DSC) values are higher than the w_c values. These findings support the assumption that the PDLLA chains were excluded from the PLLA lamellae and the inter-lamella regions. On the other hand, if PDLLA chains were trapped in the amorphous region inside the PLLA lamella stacks during crystallization process, the $\langle d \rangle$ values of blend films would become smaller than that of PLLA and decrease with decreasing X_{PLLA}, as depicted in the "Trapped model" of Fig. 12c. However, these trends contradict the obtained $\langle d \rangle$ and T_g values and, therefore, this model is excluded.

3.2.4. Spherulite morphology

Fig. 13 shows the polarized optical photomicrographs of the pure PLLA and blend films with different X_{PLLA} values isothermally crystallized at T_c of 130 °C for 10 h. For X_{PLLA} above 0.7, the normal spherulites were observed, whereas for $X_{PLLA} = 0.3$–0.5, rather disordered spherulites or crystalline assemblies were noticed. With decreasing X_{PLLA}, the number of spherulites per unit area decreased and the spherulite size increased. These findings are consistent with the previously reported results [21].

For $X_{PLLA} = 1$, the periodical extinction of spherulites along the radius direction was observed but disappeared for $X_{PLLA} = 0.9$ and 0.7, probably due to the fact that the periodical rotation of PLLA

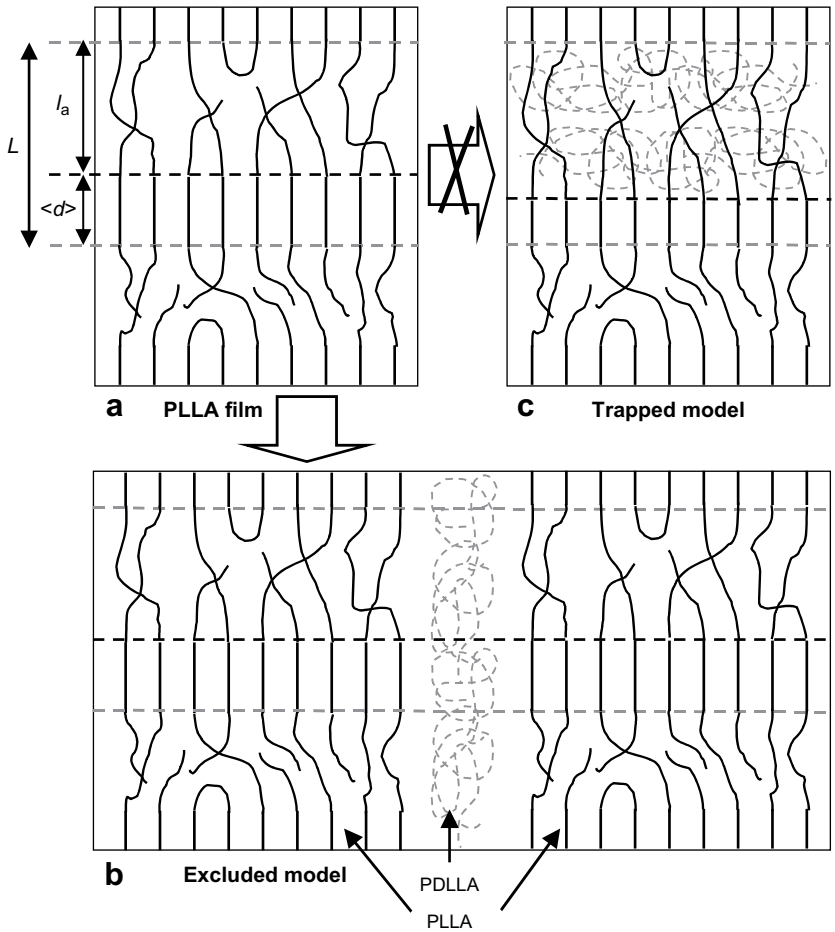

Fig. 12. Schematic representation of structures of PLLA (a) and PLLA/PDLLA blend films (excluded model) (b) and (trapped model) (c), where L is lamellae stacks of PLLA, $\langle d \rangle$ and l_a are crystalline and amorphous stack, respectively.

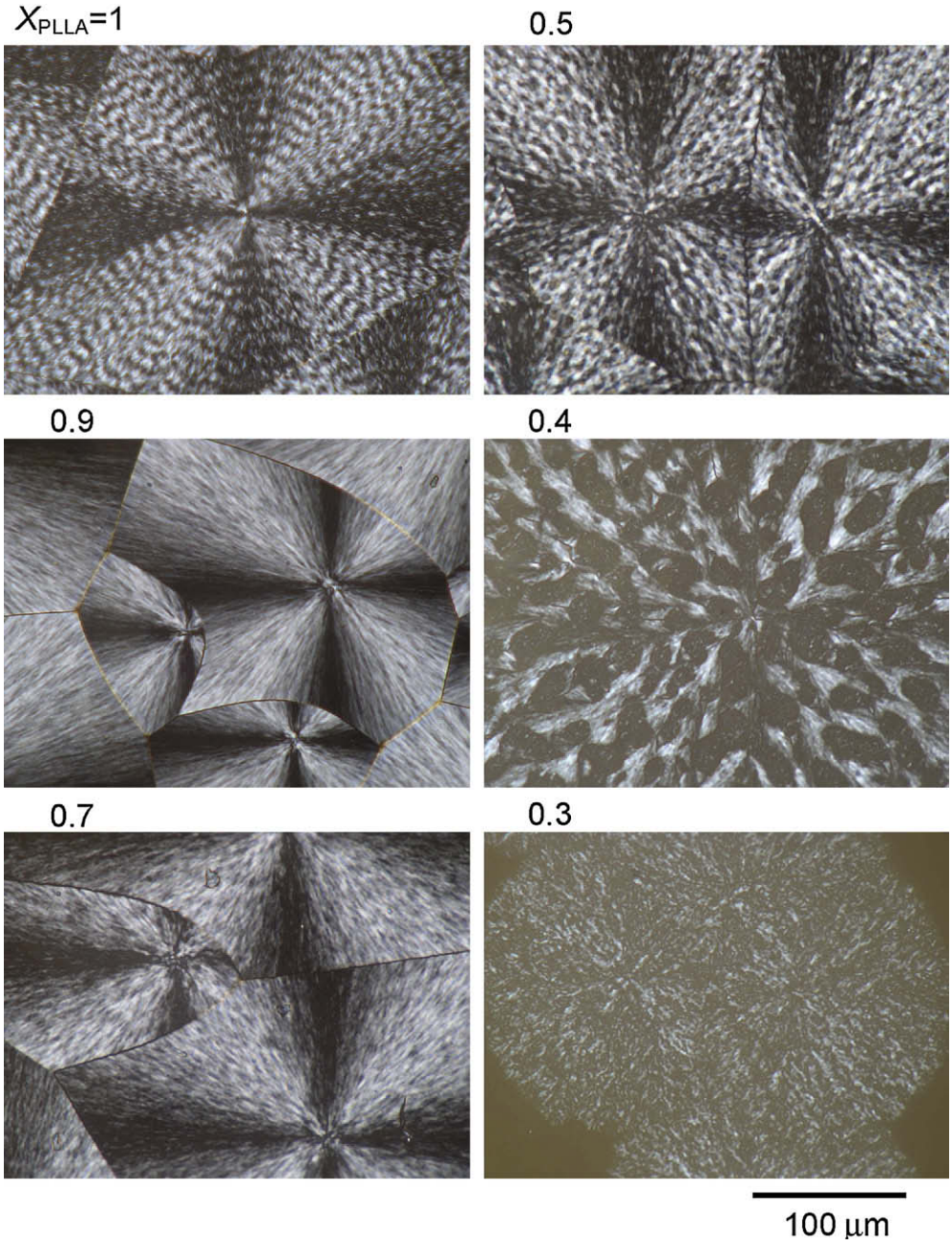

Fig. 13. Polarized photomicrographs of pure PLLA and blend films crystallized isothermally at $T_c = 130\ ^\circ C$ for 10 h.

lamellae in the spherulites was disturbed by the presence of PDLLA. For $X_{PLLA} = 0.4$ and 0.5, numerous dark spots were observed in the rather disordered spherulites or crystalline assemblies, although such spots were not seen in the spherulites or crystalline assemblies in the blend films with X_{PLLA} above 0.7. These results are indicative of the fact that the observed dark spots in the polarized photomicrographs for $X_{PLLA} = 0.4$ and 0.5 are PDLLA-rich domains. Namely, the polarized optical microscopy observable PDLLA-rich domains may have existed before crystallization and could be structurized by the rejection of PDLLA from PLLA-rich domains and assembly formation of rejected PDLLA during crystallization. Therefore, this strongly suggests that the PDLLA chains were excluded from the crystalline lamellae and inter-lamella amorphous regions during crystallization of PLLA, and the excluded PDLLA chains should have formed the amorphous domains as dark spots, and that the presence of PDLLA chains caused the disorientation of PLLA lamellae in the spherulites. On the other hand, no crystalline assemblies were formed in the pure PDLLA and blend films with $X_{PLLA} = 0$ and 0.1 (photos not shown here). This indicates that these films were amorphous, in consistent with the results obtained by DSC and WAXS measurements (Tables 1 and 2, Fig. 3) and in agreement with the reported result [21].

3.2.5. Spherulite growth

Fig. 14 shows the G and the induction period (t_i) of pure PLLA and blend films as a function of T_c. Here, we don't show the G values for $X_{PLLA} = 0.3$, because the G values were too small to be evaluated. The T_c of the PLLA and blend films with $X_{PLLA} = 0.4$–1 gave two G maxima at different T_c values of 110 and 130 °C [abbreviated as $T_{c(max)}$ values], in good agreement with the reported results by Abe

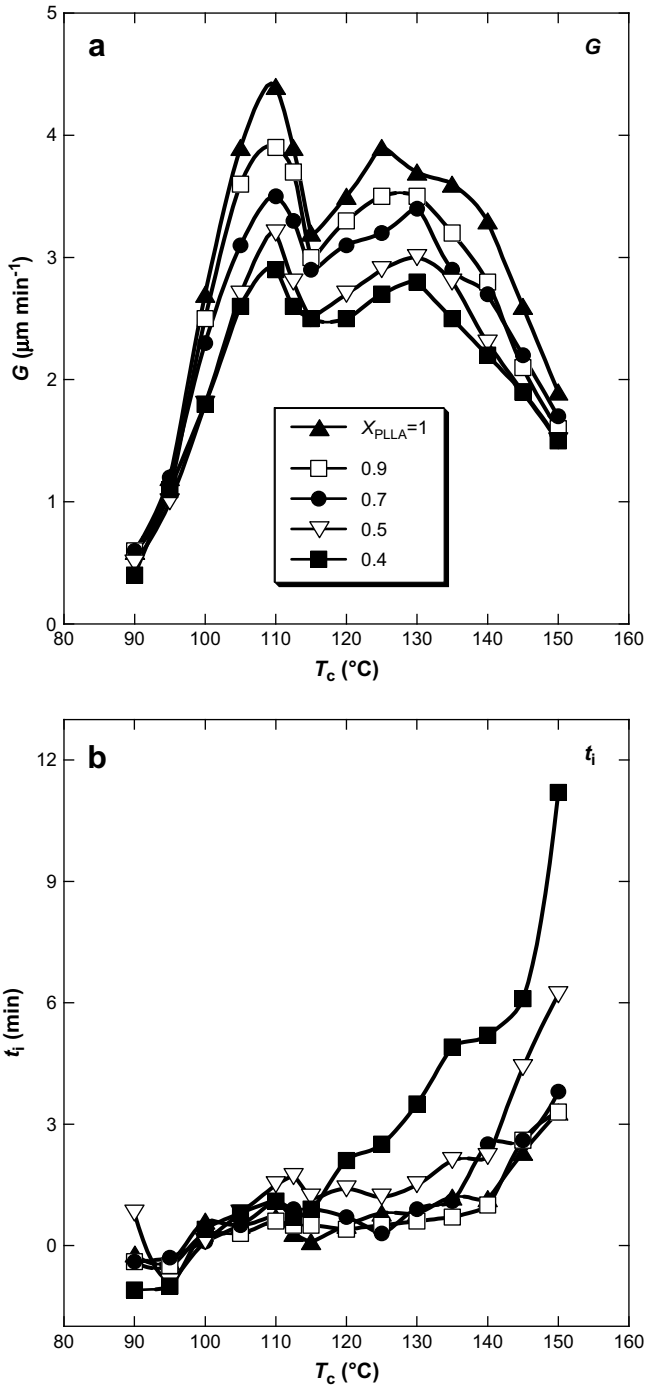

Fig. 14. Radius growth rate of spherulite (G) (a) and induction period for spherulite formation (t_i) (b) of pure PLLA and blend films as a function of T_c.

et al. [5], Di Lorenzo [11], Pan et al. [17,35], Yasuniwa et al. [12], and Yuryev et al. [37] where two maxima were observed for G curves. The formation of these two maxima can be attributed to the difference in the crystallization kinetic (regime) or the crystalline form (α'- or α-form), which transition is reported to occur at T_c values of 110 and 120 °C [9,17–19]. The shape of G curves and $T_{c(max)}$ values depend on the molecular weight of PLLA [5,9], the type and content of incorporated comonomer unit [9], tacticity [9,37], branching [8], and chain direction [10]. As seen in Fig. 14, the G of the films decreased gradually with decreasing X_{PLLA} in the T_c range of 90–150 °C, when compared at the same T_c. This is indicative of the fact that the diffusion of PLLA chains to lamella growth sites was disturbed by the very small amount of PDLLA chains present in PLLA-rich phase, which is supported by the increased T_{cc} with decreasing X_{PLLA} (Fig. 1). The decreased G may be caused by the fact that PDLLA chains were rejected and/or occluded by the spherulites growth of PLLA, as suggested by Di Lorenzo for the spherulite growth rates in binary polymer blends [36]. In the past, the effect of an incorporated immiscible amorphous polymer on the G of a crystalline polymer has been reported [38,39]. The immiscible amorphous polymers reduced G, as observed for the blends of isotactic polypropylene with ethylene–propylene [38] or ethylene–propylene–diene terpolymer [39]. Such decrease of G can be ascribed to the presence of a very small amount of the amorphous polymer in the crystalline polymer-rich phase.

On the other hand, a decrease in G was observed for poly(L-lactide-*co*-D-lactide) [P(LLA-DLA)] with a decrease in L-lactide unit content [9]. In the case of P(LLA-DLA) even the incorporation of 3.5% of D-lactide units decreased maximum G by 60%. This is marked contrast with the result in present study, where the incorporation of 30% of D-lactide units ($X_{PLLA} = 0.4$) decreased maximum G by 30% compare to that for $X_{PLLA} = 1$. Although the pure PLLA and blend films had two different $T_{c(max)}$ values of 110 and 130 °C, the copolymers had only one $T_{c(max)}$ value of 110 °C. On the other hand, the t_i values increased gradually with increasing T_c. For T_c above 120 °C, the t_i values increased with a decrease in X_{PLLA}, reflecting that the presence of PDLLA significantly disturbed the nucleation of PLLA crystallites.

4. Conclusions

From the experimental results shown above the following conclusions can be derived for the effects of incorporated PDLLA on the crystallization behavior and the spherulite growth of PLLA:

(1) In the presence of PDLLA, PLLA could crystallize and form the spherulites or crystalline assemblies for the X_{PLLA} above 0.3.
(2) PLLA and PDLLA were immiscible and phase-separated in their blend films during PLLA crystallization. PDLLA chains were excluded from the PLLA lamellae and the inter-lamella amorphous region during crystallization process.
(3) With decreasing X_{PLLA}, the G and numbers of spherulites per unit area of blend films decreased and the t_i increased. These findings are attributable to the fact that the presence of PDLLA chains should have disturbed the diffusion of PLLA chains to the growth sites of PLLA crystallites.
(4) The crystalline form of PLLA remained unvaried in the presence of PDLLA.

Acknowledgement

This research was supported by a Grant-in-Aid for Scientific Research on Priority Area, "Sustainable Biodegradable Plastics" No.11217209, and The 21st Century COE Program, "Ecological Engineering for Homeostatic Human Activities", from the Ministry of Education, Culture, Sport, Science and Technology (Japan).

References

[1] De Santis P, Kovacs A. J Biopolym 1968;6:299.
[2] Fischer EW, Sterzel HG, Wegner G, Kolloid ZZ. Polymer 1973;251:980.
[3] Kalb B, Pennings AJ. Polymer 1980;21:607.
[4] Vasanthakumari R, Pennings AJ. Polymer 1983;24:175.
[5] Abe H, Kikkawa Y, Inoue Y, Doi Y. Biomacromolecules 2001;2:1007.
[6] Miyata T, Masuko T. Polymer 1998;39:5515.
[7] Wang Y, Mano JF. J Appl Polym Sci 2007;105:3500.
[8] Tsuji H, Miyase T, Tezuka Y, Saha S-K. Biomacromolecules 2005;6:244.
[9] Tsuji H, Tezuka Y, Saha S-K, Suzuki M, Itsuno S. Polymer 2005;46:4917.

[10] Tsuji H, Sugiura Y, Sakamoto Y, Bouapao L, Itsuno S. Polymer 2008;49:1385.
[11] Di Lorenzo ML. Eur Polym J 2005;41:569.
[12] Yasuniwa M, Tsubakihara S, Iura K, Ono Y, Dan Y, Takahashi K. Polymer 2006; 47:7554.
[13] Zhang J, Tsuji H, Noda I, Ozaki Y. J Phys Chem B 2004;108:11514.
[14] Zhang J, Tsuji H, Noda I, Ozaki Y. Macromolecules 2004;37:6433.
[15] Huang J, Lilowski MS, Runt J. Macromolecules 1998;31:2593.
[16] Tsuji H, Ikarashi K, Fukuda N. Polym Degrad Stab 2004;84:515.
[17] Pan P, Zhu B, Kai W, Dong T, Inoue Y. J Appl Polym Sci 2008;107:54.
[18] Kawai T, Rahma N, Matsuba G, Nishida K, Kanaya T, Nakano M, et al. Macromolecules 2007;40:9463.
[19] Zhang J, Tashiro K, Tsuji H, Domb AJ. Macromolecules 2007;40:1049.
[20] Yasuniwa M, Sakamo K, Ono Y, Kawahara W. Polymer 2008;49:1943.
[21] Tsuji H, Ikada Y. J Appl Polym Sci 1995;58:1793.
[22] Tsuji H, Ikada Y. Polymer 1996;37:595.
[23] Tsuji H, Ikada Y. J Appl Polym Sci 1997;63:855.
[24] Ren J, Adachi K. Macromolecules 2003;36:5180.
[25] Xu J, Guo BH, Zhou JJ, Li L, Wu J, Kowalczuk M. Polymer 2005;46:9176.
[26] Urayama H, Kanamori T, Kimura Y. Macromol Mater Eng 2002;287:116.
[27] Chen CC, Chueh JY, Tseng H, Huang HM, Lee SY. Biomaterials 2003;24:1167.
[28] Jorda R, Wilkes GL. Polym Bull 1988;20:479.
[29] Tsuji H, Ikada Y. Polym Degrad Stab 2000;67:179.
[30] Tsuji H, Nakahara K, Ikarashi K. Macromol Mater Eng 2001;286:398.
[31] Stroblb GR, Schneider M. J Polym Sci Polym Phys Ed 1980;18:1343.
[32] Stroblb GR, Schneider M, Voigt-Martin IG. J Polym Sci Polym Phys Ed 1980;18:1361.
[33] Baratian S, Hall ES, Lin JS, Xu R, Runt J. Macromolecules 2001;34:4857.
[34] Cho J, Baratian S, Kim J, Yeh F, Hsiao BS, Runt J. Polymer 2003;44:711.
[35] Pan P, Kai W, Zhu B, Dong T, Inoue Y. Macromolecules 2007;40:6898.
[36] Di Lorenzo ML. Prog Polym Sci 2003;28:663.
[37] Yuryev Y, Wood-Adams P, Heuzey MC, Dubois C, Brisson J. Polymer 2008;49: 2306.
[38] Yokoyama Y, Ricco J. Appl Polym Sci 1997;66:1007.
[39] Martuscelli E. Polym Eng Sci 1984;24:563.